Size effects in energy transport between thermal contacts mediated by nanoparticles

George Y. Panasyuk,[1,2,*] Kirk L. Yerkes,[1] and Timothy J. Haugan[1]

[1]*Aerospace Systems Directorate, Air Force Research Laboratory, Wright-Patterson Air Force Base, Ohio 45433, USA*
[2]*UES, Inc., 4401 Dayton-Xenia Road, Dayton, Ohio 45432, USA*

We investigate size effects in phononic energy transport in a system of two nanoparticles interconnected by a molecule and attached to thermal contacts also by molecules. In the considered closed system, the nanoparticles and contacts are described by ensembles of finite numbers of harmonic oscillators within the Drude-Ullersma model. The macroscopic character of the contacts is simulated by a large value of the ratio $\Delta/\Delta_B = n \, (n > 100)$ of mode spacings Δ and Δ_B corresponding to the nanoparticles and contacts, respectively. Quasistatic energy transport on the timescale Δ^{-1} is investigated. Equations describing the dynamics of the averaged eigenmode energies that belong to the nanoparticles and contacts are derived and solved. The resulting expressions for the energy current exiting (entering) the contacts as well as the energy current between the nanoparticles are obtained and investigated. The latter current accounts for energy accumulation by (depletion from) the nanoparticles. The finite size effects result in reversibility features and peculiarities at time moments $t = 2\pi\ell\Delta^{-1}$ for non-negative integers ℓ. They are qualitatively the same as in a previously studied system of two equal nanoparticles mediated by a molecule, despite the presence of the macroscopic contacts. The thermal conductance of the whole nanojunction is derived and explored. The energy currents and thermal conductance of the nanojunction in a case when its parameters are known from the experiment are computed using the developed model.

I. INTRODUCTION

Understanding the mechanisms of how energy (heat) transfers through microscopic systems, such as molecules, nanoparticles, or nanotubes, is one of the most important research directions in modern physics and technology. However, because of the necessity to account for quantum properties and the nonequilibrium character of the problem [1–3], this research still encounters many problems. In addition, due to miniaturization of electronic devices and the increasing density of binary switches in computer systems, development of a fundamentally new approach to manipulate heat flow has become increasingly important [4–6]. Indeed, the ultimate physical limit of integration in integrated circuitry is power dissipation [4,5]. Research suggests [7–13] that molecular and nanoscale systems may also be good candidates for many technological advances, such as thermoelectrics, molecular diodes, switches, rectifiers, and quantum heat transfer in anharmonic junctions.

An important approach to deal with energy transport through microscopic systems is based on the quantum Langevin equation [14,15]. It was used, in particular, for studying the thermalization of a quantum particle coupled harmonically to a thermal reservoir [16,17] and to explore the steady-state heat current and temperature profiles in chains of harmonic oscillators placed between two thermal baths [18–21]. Closely related to the Langevin dynamics is a "quantum thermal bath method" [22,23] that was successfully used for sampling quantum fluctuations within the framework of

molecular dynamics (MD) and for reproducing the quantum Wigner distribution of a variety of model potentials. A similar approach was developed in [24], allowing to avoid direct MD simulation. Based on classical MD, the method employs a coarse-graining procedure adopting the statistical-operator approach [25] and the classical linear response theory [26]. Another frequently used approach is the nonequilibrium Green's function (NEGF) method [27]. It was applied to calculate electron transport and steady-state properties of a finite system interconnecting reservoirs modeled by noninteracting Hamiltonians with infinite degrees of freedom [28–30] and to phonon transport [31–36]. However, for systems represented by harmonic oscillators, the Langevin approach reproduces the NEGF results exactly [2,37]. Recently, a new method for exactly solving the Lindblad and Redfield master equations, which can be considered as an alternative to the quantum Langevin equation, was developed [38–40].

In the above-mentioned studies the thermal reservoirs were considered in the thermodynamic limit, i.e., having an infinitely large number of modes. However, due to scaling down of electronic devices, size effects related to finite numbers of atoms in nanosize components of such devices have become increasingly important. For this reason, the study of size effects in nanostructured materials became an important part of modern research. While study of the size and quantum effects in the electromagnetic response of nanoparticles has a rather long history [41–45], exploration of the role of size effects in thermal properties of small particles has taken place only recently. In particular, in [46–48], the static thermodynamic properties of nanostructures, such as the local structure of the grain boundary in ultrananocrystals, the phonon density of states in nanostructures, and the order-disorder transition

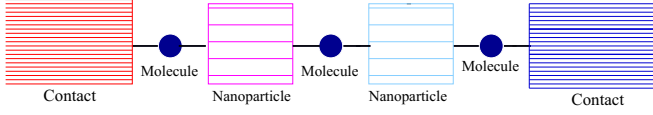*george.panasyuk.1.ctr@us.af.mil

032141-1

FIG. 1. Diagram representation of the nanojunction under consideration. The macroscopic character of the contacts is expressed by dense eigenstate levels.

in nanoparticles were investigated. An idea of a possible recurrent behavior in a system with a quantum particle coupled to a harmonic quantum thermal bath was mentioned in [17] (however, without any further analysis). In [49], the authors found a recurrent phenomenon in the time evolution of the energy current in a finite linear chain showing the critical role of the on-site pinning potential in establishing quasi-steady-state conditions. Finally, finite-size effects on energy current in a system of two nanoparticles interconnected by a molecule were explored in [50,51].

In this work, we study phononic quasistatic energy transport on the timescale $t \sim \Delta^{-1} \ll \Delta_{\mathrm{B}}^{-1}$ between thermal reservoirs (contacts) connected by molecules to a system of two equal nanoparticles interconnected also by a molecule (see Fig. 1). Here Δ and Δ_{B} are the mode spacing constants for the nanoparticles and contacts, respectively. Our major goal is to study finite size effects, related to small but nonzero Δ (or a finite number of atoms in the nanoparticles), on the energy current between the nanoparticles and on the energy current that exits or enters the contacts. Unlike the nanoparticles, the contacts are considered as macroscopic bodies and their macroscopic nature is simulated by a large ratio, $\Delta/\Delta_{\mathrm{B}}$. Our previous work [50] revealed finite size effects, such as peculiarities at time moments $t = 2\pi\ell/\Delta$ with integers $\ell \geqslant 0$ and quasiperiodicity features, in a system of two equal nanoparticles connected by a molecule. In this regard, this work is a more realistic generalization of [50], because in any device any nanostructured feature is connected to the device's macroscopic part. Another goal is to derive the thermal conductance of the nanojunction and compute it, together with the energy currents, for a case when the nanojunction's parameters are known from an experiment.

The paper is organized as follows. The model is introduced in Sec. II, where the eigenstates of the whole system are found and solutions for the displacement operators of the molecules are obtained. In Sec. III, equations governing the dynamics of the eigenmode average energies together with the expressions for the energy currents and thermal conductance of the chain are derived. In Sec. IV, the derived equations are approximately solved and the energy currents together with the thermal conductance of the nanojunction are computed. Finally, Sec. V provides a summary to our research and discusses a possible experimental realization for a system of this kind.

II. MODEL

The total Hamiltonian of the system under consideration, illustrated in Fig. 1, is a generalization of that in

Refs. [21,50,52,53]:

$$\mathcal{H}_{\mathrm{tot}} = \mathcal{H}_{\mathrm{BL}} + \mathcal{H}_{\mathrm{BR}} + \mathcal{H}_{\mathrm{n1}} + \mathcal{H}_{\mathrm{n2}} + \mathcal{H}_{\mathrm{ML}}$$
$$+ \mathcal{H}_{\mathrm{MR}} + \mathcal{H}_{\mathrm{MC}} + \mathcal{V}_{\mathrm{1M}} + \mathcal{V}_{\mathrm{2M}} + \mathcal{V}_{\mathrm{BL}} + \mathcal{V}_{\mathrm{BR}}. \quad (1)$$

Here

$$\mathcal{H}_{\mathrm{M}\sigma} = \frac{p_\sigma^2}{2m_\sigma} + \frac{k_\sigma x_\sigma^2}{2}, \quad \sigma = \mathrm{C}, \ \mathrm{L}, \ \mathrm{R} \quad (2)$$

are the Hamiltonians of the central, left, and right molecules,

$$\mathcal{H}_{\mathrm{B}\mu} = \sum_{i=1}^{N_\mu} \left[\frac{p_{\mu i}^2}{2m_{\mu i}} + \frac{m_{\mu i}\omega_{\mu i}^2 x_{\mu i}^2}{2} \right], \quad \mu = \mathrm{L}, \ \mathrm{R}, \quad (3)$$

are the Hamiltonians of the thermal reservoirs having N_μ quantum oscillators (modes),

$$\mathcal{H}_{\mathrm{n}\nu} = \sum_{i=1}^{N_\nu} \left[\frac{p_{\nu i}^2}{2m_{\nu i}} + \frac{m_{\nu i}\omega_{\nu i}^2 x_{\nu i}^2}{2} \right], \quad \nu = 1, \ 2, \quad (4)$$

are the Hamiltonians of the nanoparticles having N_ν modes,

$$\mathcal{V}_{\mathrm{B}\mu} = -x_\mu \sum_{i=1}^{N_\mu} C_{\mu i} x_{\mu i} + x_\mu^2 \sum_{i=1}^{N_\mu} \frac{C_{\mu i}^2}{2m_{\mu i}\omega_{\mu i}^2}, \quad (5)$$

where $\mu = \mathrm{L}, \ \mathrm{R}$, describe interaction between the left and right contacts and the corresponding molecules,

$$\mathcal{V}_{\nu \mathrm{M}} = -\sum_{i=1}^{N_\nu} \hat{C}_{\nu i} x_{\nu i} + \sum_{i=1}^{N_\nu} \frac{\hat{C}_{\nu i}^2}{2m_{\nu i}\omega_{\nu i}^2}, \quad (6)$$

with $\hat{C}_{1i} = C_{1i}x_{\mathrm{C}} + C_{1i}'x_{\mathrm{L}}$, when $\mathcal{V}_{\mathrm{1M}}$ describes interaction between the first (left) nanoparticle and the central and left molecules, and $\hat{C}_{2i} = C_{2i}x_{\mathrm{C}} + C_{2i}'x_{\mathrm{R}}$, when $\mathcal{V}_{\mathrm{2M}}$ describes interaction between the second (right) nanoparticle and the central and right molecules. Quadratic terms in Eqs. (5) and (6) are added in order to make $\mathcal{H}_{\mathrm{tot}}$ positively defined. In Eq. (2), x_σ and p_σ are the displacement and momentum operators and m_σ and k_σ are the masses and the spring constants of the molecules. In Eqs. (3) and (5), $x_{\mu i}$ and $p_{\mu i}$ are the displacement and momentum operators, whereas $m_{\mu i}$ and $\omega_{\mu i}$ are the masses and frequencies of the contacts' oscillators in the absence of interaction with the molecules. In (4) and (6), $x_{\nu i}$, $p_{\nu i}$, $m_{\nu i}$, and $\omega_{\nu i}$ are the similar quantities for the nanoparticles. Finally, $C_{\mu,\nu i}$ and $C_{\nu i}'$ are the coupling coefficients that describe interaction between the contacts or nanoparticles with the adjacent molecules. In order to make our description quantitative, we employ the Drude-Ullersma model [16,17,54,55] that assumes that in the absence of interaction with the molecules, each contact and nanoparticle consist of uniformly spaced modes and introduces the following frequency dependence for the coupling coefficients:

$$\omega_{\epsilon i} = i\Delta_\epsilon, \quad C_{\epsilon i} = \sqrt{\frac{2\gamma_\epsilon m_{\epsilon i}\omega_{\epsilon i}^2 \Delta_\epsilon D_\epsilon^2}{\pi(\omega_{\epsilon i}^2 + D_\epsilon^2)}}. \quad (7)$$

When $\epsilon = \mu = \mathrm{L}$ or R, $i = 1, 2, ...N_\mu$ and D_μ, Δ_μ, and γ_μ are the Debye cutoff frequencies for the left or right contacts, the mode spacing constants for the contacts, and the coupling constant between a given contact and the adjacent molecule, respectively. When $\epsilon = \nu = 1$ or 2, $i = 1, 2, ...N_\nu$ and D_ν,

Δ_ν are the similar quantities for the nanoparticles, whereas γ_ν is the coupling constant between a given nanoparticle and the central molecule. The coupling coefficients C'_{1i} and C'_{2i} describe interaction between the first (second) nanoparticle and left (right) molecule. They are determined by relation $C'_{\nu i} = C_{\nu i}(\gamma \to \gamma') = \sqrt{\gamma'_\nu/\gamma_\nu}\, C_{\nu i}$.

Despite that the analytical derivation shown below can be done for any values of the chain parameters, in order to facilitate numerical study we assume that (i) the left and right molecules are identical, having the same masses $M_L = M_R \equiv M$ and fundamental frequencies $\Omega_L = \Omega_R \equiv \Omega$; (ii) the nanoparticles are made of the same material:

$$D_1 = D_2 \equiv D, \quad \gamma_1/m = \gamma_2/m \equiv \gamma/m \equiv \hat{\gamma}, \quad (8)$$

where $m_C \equiv m$ and $\omega_C \equiv \omega$ are the mass and fundamental frequency of the central molecule, respectively; and (iii) the contacts are made of the same material:

$$D_L = D_R \equiv D_B, \quad \gamma_L/M = \gamma_R/M \equiv \gamma_B/M \equiv \hat{\gamma}_B. \quad (9)$$

In addition, we assume that the nanoparticles are equal:

$$\Delta_1 = \Delta_2 \equiv \Delta, \quad N_1 = N_2 \equiv N = \omega_m/\Delta, \quad (10)$$

where ω_m is the maximum frequency in the nanoparticle spectrum. In order to simulate the macroscopic nature of the contacts, we assume that

$$\Delta_L = \Delta_R \equiv \Delta_B \ll \Delta; \quad N_L = N_R \equiv N_B = \omega_{Bm}/\Delta_B, \quad (11)$$

where $N_B \gg N$ and ω_{Bm} is the maximum frequency in the contacts' spectrum. As one can suppose, there is no need to distinguish between the mode numbers in the contacts, due to N_L, $N_R \to \infty$, and we introduce only one mode number N_B for both contacts. Also, due to the dense character of the undisturbed contacts' spectrum compared to the undisturbed nanoparticles' spectrum, we assume that each frequency in the nanoparticle spectrum "hits" some frequency in the contact spectrum: $\Delta/\Delta_B = n$, where $n \gg 1$ is an integer. With these simplifications, we can drop the indexes μ and ν in $C_{\mu i}$, $C_{\nu i}$, $C'_{\nu i}$, and r_ν, denoting them as C_{Bi}, C_i, C_{ri}, and $r \equiv \sqrt{\gamma'/\gamma}$, respectively.

Our major goal is to consider temporal variations of all variables on the timescale Δ^{-1}, which is much longer than the microscopic time

$$\tau = \max\left[\hat{\gamma}^{-1}, (\hat{\gamma}')^{-1}, \hat{\gamma}_B^{-1}, \omega^{-1}, \Omega^{-1}, D^{-1}, D_B^{-1}\right], \quad (12)$$

determining transient processes. So, we have

$$\tau \ll \Delta^{-1} \lesssim t \ll \Delta_B^{-1}. \quad (13)$$

In the first step, we find the eigenstates (eigenmodes) of our chain (see Appendix A). As a result, our roots z_k (eigenfrequencies of the chain) can be presented as the unification

$$\{z_k\}_{k=1}^{N_{tot}} = \{z_{Bk}\}_{k=1}^{N_B} \bigcup \{z_{nk}\}_{k=1}^{N} \quad (14)$$

of two subsets: the first is the roots associated with the contacts and second is the roots associated with the nanoparticles. In both cases, each root can be presented as

$$z_k = k\Delta_B - \phi_k \Delta_B, \quad k = 1, 2, ..., N_{tot} = N_B + N, \quad (15)$$

where $|\phi_k| \lesssim 1$. Thus, the first and second subsets of the roots are slightly but inhomogeneously shifted from the sets

of the uniformly spaced modes that belong to the contacts and nanoparticles, respectively, before interconnecting them by the molecules. It is worth mentioning that none of the nanoparticles' roots coincide with any contacts' root, despite our assumption written after Eq. (11). This makes it possible to clearly distinguish between the dynamics of the eigenmode average energies of the nanoparticles and contacts and derive unambiguous expressions for the energy currents that enter or exit the contacts and between the nanoparticles. In the second important step, we find temporal solutions for all operators that encounter (1) (see Appendix A) and are used to describe the dynamics of our system on the timescale Δ^{-1}.

III. QUASISTATIC ENERGY BALANCE

Taking into account that our time-dependent variables satisfy the Heisenberg equations, one can find the rate of change of the averaged energy E_μ of the μth contact:

$$\sum_{i=1}^{N_B} \left\langle \frac{d}{dt}\left(\frac{p_{\mu i}^2}{2m_{Bi}} + \frac{m_{Bi}\omega_{Bi}^2 x_{\mu i}^2}{2}\right)\right\rangle$$
$$= \sum_{i=1}^{N_B} \frac{C_{Bi}}{2m_{Bi}}\langle p_{\mu i}x_\mu + x_\mu p_{\mu i}\rangle \equiv \mathcal{P}_{B\mu}, \quad \mu = L, R, \quad (16)$$

where the angular brackets denote the ensemble averaging (see below) and $\mathcal{P}_{B\mu}$ is the work per unit of time performed by the left (right) molecule over the left (right) contact (or the corresponding power dissipated in the left or right contacts [18]). In a similar way, one finds that the rate of change of the energy E_ν of the νth nanoparticle is

$$\sum_{i=1}^{N} \left\langle \frac{d}{dt}\left(\frac{p_{\nu i}^2}{2m_i} + \frac{m_i\omega_i^2 x_{\nu i}^2}{2}\right)\right\rangle \equiv \mathcal{P}_{C\nu} + \mathcal{P}_{\mu(\nu)\nu}, \quad (17)$$

where $\nu = 1, 2$. Here

$$\mathcal{P}_{C\nu} = \sum_{i=1}^{N} \frac{C_i}{2m_i}\langle p_{\nu i}x_C + x_C p_{\nu i}\rangle \quad (18)$$

is the work per unit of time performed by the central molecule over the νth nanoparticle, and

$$\mathcal{P}_{\mu(\nu)\nu} = \sum_{i=1}^{N} \frac{C_{ri}}{2m_i}\langle p_{\nu i}x_{\mu(\nu)} + x_{\mu(\nu)}p_{\nu i}\rangle \quad (19)$$

is the work per unit of time performed by the left (right) molecule over the first (second) nanoparticle.

As was shown [17], after coupling of a quantum particle to a thermal reservoir, the whole system comes to equilibrium after a microscopic time τ. Similar to [17] and [50], in our case of two contacts and nanoparticles having different initial temperatures, small energy currents, provided by "narrow" channels of the molecular bridges, will be established during the time τ (12) after connecting of the chain. One can assume that in each moment of time each nanoparticle and contact has a quasiequilibrium density matrix with slowly changing parameters. More accurately, after the diagonalization and introducing the eigenmode creation and annihilation operators $a_{\epsilon k}^+$ and $a_{\epsilon k}$, where $\epsilon = \mu = L, R$ or $\epsilon = \nu = 1, 2$, one can present the density matrix of the whole system in

the form $\rho_\epsilon \sim \exp[-\sum_k \beta_{\epsilon k} z_k(a_{\epsilon k}^+ a_{\epsilon k} + 1/2)]$, similar to [50] with $\beta_{\epsilon k}(t) = 1/k_B T_{\epsilon k}(t)$. Here, instead of trying to determine the eigenmode temperatures $T_{\epsilon k}(t)$, we will construct and solve equations to determine the (slow) dynamics of eigenmode average energies $E_{\epsilon k} = E_{\epsilon k}(t)$ and, eventually, energy currents on the timescale (13) (see Appendix B).

In general, averaged energies $E_{\nu,\mu}$ of the νth nanoparticle and the μth contact will consist of contributions from all the eigenmodes. On the other hand, similar to [51], it is natural to expect that shortly after interconnecting of the chain, E_ν will be presented mostly by contributions $E_{\nu k}^n$ from the $\{z_{nk}\}|_{k=1}^N$ subset of the eigenmodes. It will contain also small contributions $E_{\nu k}^B$ from the $\{z_{Bk}\}|_{k=1}^{N_B}$ subset. In the same way, E_μ will be presented mostly by contributions $E_{\mu k}^B$ from the $\{z_{Bk}\}|_{k=1}^{N_B}$ subset, also having small contributions $E_{\mu k}^n$ from the $\{z_{nk}\}|_{k=1}^N$ subset. Because neither a nanoparticle nor a contact temperatures can change noticeably over τ, one can assume that at $t = 0$,

$$E_{\nu k}^n(0) = \frac{\hbar z_{nk}}{2} \coth \frac{\hbar z_{nk}}{2k_B T_\nu} \quad \text{and} \quad E_{\nu k}^B(0) = 0, \quad (20)$$

$$E_{\mu k}^B(0) = \frac{\hbar z_{Bk}}{2} \coth \frac{\hbar z_{Bk}}{2k_B T_\mu} \quad \text{and} \quad E_{\mu k}^n(0) = 0, \quad (21)$$

and $T_{\nu,\mu}$ are initial (equilibrium) temperatures of the nanoparticles ($\nu = 1, 2$) and contacts ($\mu = L, R$), respectively. As follows from (20), (21), and (B10)–(B13), the only equations that we need to solve are (see Appendix B)

$$\frac{d}{dt}\big[E_{Lk}^B(t) - E_{Rk}^B(t)\big] = F_{Bk}\big[E_{Lk}^B(t) - E_{Rk}^B(t)\big] \quad (22)$$

if $z_k \in \{z_{Bk}\}_{k=1}^{N_B}$, and

$$\frac{d}{dt}\big[E_{1k}^n(t) - E_{2k}^n(t)\big] = (F_{nk}' + F_{nk}'')\big[E_{1k}^n(t) - E_{2k}^n(t)\big] \quad (23)$$

if $z_k \in \{z_{nk}\}_{k=1}^N$. The other energy differences vanish,

$$E_{Lk}^n(t) - E_{Rk}^n(t) = E_{1k}^B(t) - E_{2k}^B(t) \equiv 0, \quad (24)$$

due to second relations in (20) and (21). These observations lead us to the following expression for energy current flowing between the nanoparticles (see Appendix B),

$$J^{(12)}(t) = J_B^{(12)}(t) + J_n^{(12)}(t), \quad (25)$$

where

$$J_B^{(12)}(t) = -\frac{1}{2} \sum_{k=1}^{N_B} F_{Bk}\big[E_{Lk}^B(t) - E_{Rk}^B(t)\big] = J_B^{(LR)}(t) \quad (26)$$

is also the energy current exiting from the left contact or entering the right contact, and

$$J_n^{(12)}(t) = -\frac{1}{2} \sum_{k=1}^N (F_{nk}' + F_{nk}'')\big[E_{1k}^n(t) - E_{2k}^n(t)\big] \quad (27)$$

is its modification due to energy absorbed by (or depleted from) the left nanoparticle. Assuming continuity of the eigenmode average energies $E_{\mu,\nu k}^{B,n}$ as functions of time (otherwise $\frac{d}{dt}E_{\mu,\nu k}^{B,n}(t)$ will diverge at $t = 2\pi \ell/\Delta$, when $\ell = 0, 1, 2, ...$) and taking into account initial conditions (20)–(21), Eqs. (22) and (23) can be solved and all currents can be computed.
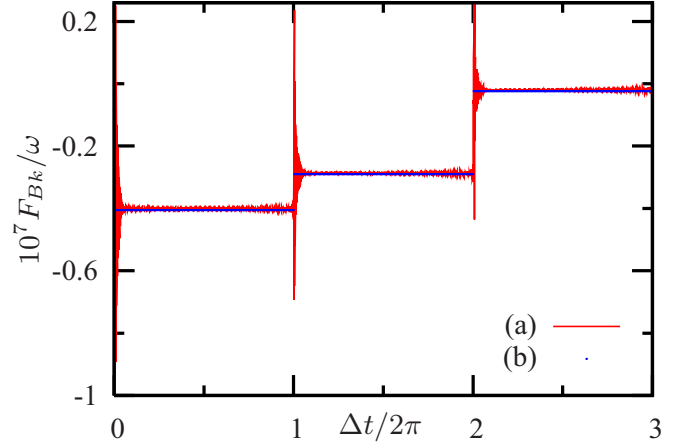

FIG. 2. Time dependences of F_{Bk} when $\hat{\gamma}/\omega = 0.1$, $D/\omega = 1$, $\Delta/\omega = 0.001$, and $k = 10^5$: (a) accurate result and (b) its approximation by a sequence of step functions.

Finally, for $\Delta T = T_L - T_R \to 0$, one finds the thermal conductance K of the chain:

$$K = \frac{J_B^{(LR)}}{\Delta T} = \frac{1}{2} \sum_{k=1}^{N_B} F_{Bk} \frac{s^2}{\sinh^2(s)}, \quad s \equiv \frac{\hbar z_k}{2k_B T_{av}}, \quad (28)$$

and $T_{av} = (T_L + T_R)/2$; we assumed for clarity that $T_L > T_R$.

For just two equal nanoparticles connected by a molecule, all coefficients F are zeros except F_{nk}', so the energy current between the nanoparticles in this case is

$$J_0^{(12)}(t) = -\frac{1}{2} \sum_{k=1}^N F_{nk}'\big[E_{1k}^n(t) - E_{2k}^n(t)\big], \quad (29)$$

where only the nanoparticle eigenmodes $\{z_{nk}\}_{k=1}^N$ must be taken into account. They are found by solving the equation $h = 0$, where h is determined in (A1) with $C_r = 0$.

IV. RESULTS AND DISCUSSION

In the numerical examples considered here, we assume, in addition to Eqs. (8)–(11), that all the molecules in the chain are identical and the nanoparticles are made of the same material as the contacts, resulting in $\hat{\gamma}_B = \hat{\gamma}' = \hat{\gamma}$, $m = M$, and $\omega = \Omega$. As in [50], we choose $\omega_m = \omega_{Bm} = 1.3D$ and $N = 1300$.

As follows from our numerical analysis, the coefficients F can be approximated by a sequence of step functions with the steps occurring at $t = \ell P$, $\ell = 0, 1, 2,...$, and the value of each coefficient on an interval $\ell P \leqslant t \leqslant (\ell + 1)P$ is equal to its time average on the interval (see Fig. 2 for F_{Bk} coefficient). The accuracy of this approximation was checked by computing ratios $|D_{k1}|$ and $|D_{k2}|$ to their largest values in the right-hand sides of (B15) and (B16), respectively, for each k and were found to be about several percent, supporting this approximation for the F and R coefficients (Appendix B). It is also in line with our goal to describe the dynamics on the timescale $\Delta^{-1} \gg \tau$, i.e., disregarding details of transient processes. This allows analytical solutions of Eqs. (22) and (23) on each interval $\ell P \leqslant t \leqslant (\ell + 1)P$. Due to the
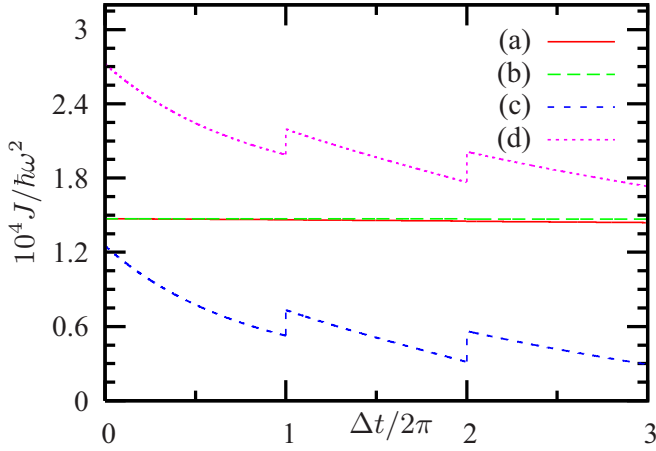
FIG. 3. Time dependences of (a) $J_B^{(LR)}(t)$ and (b) its approximation $J_B^{(LR)}(0)$; (c) energy current $J_n^{(12)}(t)$ and (d) total energy current (25) between the nanoparticles; $T_L = 300$ K.

step-function approximation, some curves in Figs. 3–8 possess "jumps" (sharp changes).

In Figs. 3–6, $\Delta/\omega = 0.001$, $\Delta_B/\omega = 7.8 \times 10^{-6}$, $N_B = 1.7 \times 10^5$, $\alpha \equiv (T_L - T_R)/T_L = 0.01$, and we assumed that $T_1 = T_L(1 - \alpha/3)$ and $T_2 = T_L(1 - 2\alpha/3)$. It is important, however, to notice that our approach is valid even for $\alpha \sim 1$. In Figs. 3 and 4, $D/\omega = 1$ and $\hat{\gamma}/\omega = 0.1$.

Due to the extensity of the contacts ($N_B \gg N$), one can neglect temporal variation of their eigenenergies, approximating

$$E_{Lk}^B(t) \approx E_{Lk}^B(0) \text{ and } E_{Rk}^B(t) \approx E_{Rk}^B(0), \quad (30)$$

where $E_{L,Rk}^B(0)$ are determined by (21). This approximation is supported in Figs. 3–6, in which curves (b) show approximate (time independent) $J_B^{(LR)}$ from (26) using (30).

Figures 5 and 6 predict this kind of time dependence when all contacts and nanoparticles are made of silicon with $D = D_B = 457$ cm^{-1} interconnected by SiO$_2$ molecules having $\omega = \Omega = 460$ cm^{-1} [56], which corresponds to $\Delta^{-1} \sim 100$ ps and $\hat{\gamma}/\omega \approx 0.16$. The latter quantity was estimated from the FWHM of the corresponding absorption experiment [56].

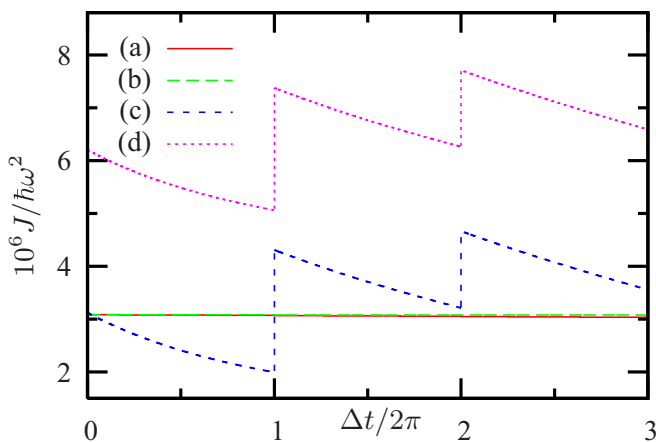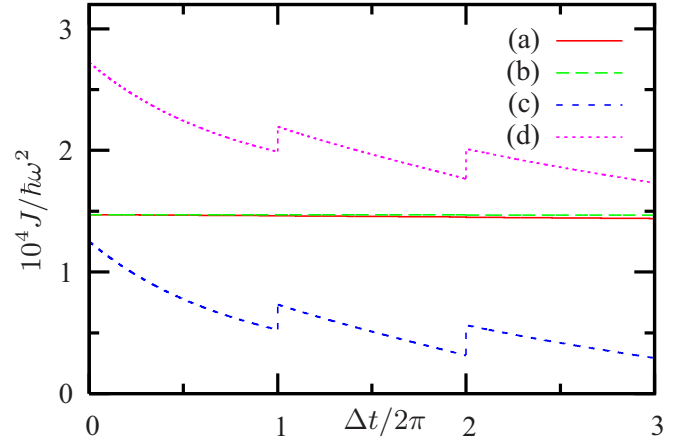An important consequence of the presented results is that the total energy currents $J^{(12)}(t)$ between the nanoparticles essentially repeat the shapes of their partial contributions $J_n^{(12)}(t)$, shifting their values by the approximately constant "background" currents $J_B^{(LR)}(t)$ that exit (enter) the contacts. Figures 7 and 8 show energy currents $J_0^{(12)}(t)$ between the same nanoparticles in the absence of the contacts at the same parameters ω_m, N, ω, and $\hat{\gamma}$ as in the "contact" case. As one finds, the currents $J_n^{(12)}(t)$ shown in Figs. 3–6 are qualitatively similar to the corresponding currents in Figs. 7 and 8, demonstrating the same quasiperiodicity. It is important to note that as presented in Figs. 3–6, temporal dependencies are valid only for $t \ll \Delta_B^{-1}$, when one can consider the contacts having essentially infinite sizes.

Using Eq. (28), one can compute the thermal conductance K for the total nanojunction chain and compare it to the corresponding thermal conductance K_0 obtained for a nanojunction that consists of only two macroscopic contacts interconnected by a molecule [53] (no nanoparticles). In the experimental case [56], when $\hat{\gamma}/\omega = 0.16$, results are the following: if $T = 300$ K, $K/k_B\omega = 1.1 \times 10^{-2}$ and $K_0/k_B\omega = 0.06$; if $T = 100$ K, $K/k_B\omega = 1.1 \times 10^{-3}$ and $K_0/k_B\omega = 1.4 \times 10^{-3}$; if $T = 50$ K, $K/k_B\omega = 8.4 \times 10^{-5}$ and $K_0/k_B\omega = 1.8 \times 10^{-4}$.

FIG. 5. Same as in Fig. 3 for $T_L = 300$ K and $\hat{\gamma}/\omega = 0.16$.

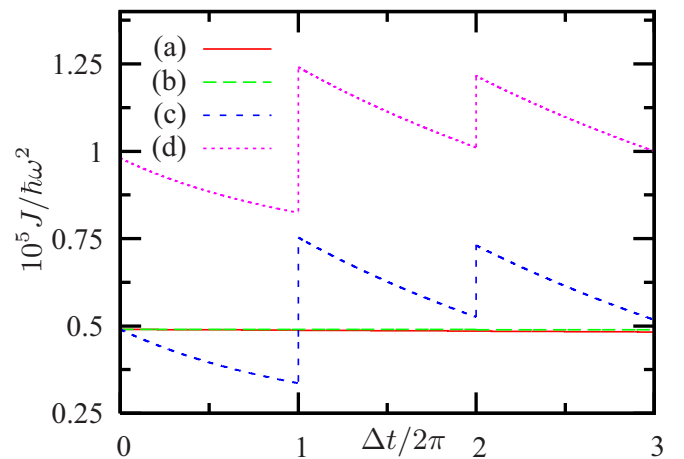FIG. 4. Same as in Fig. 3 for $T_L = 100$ K.

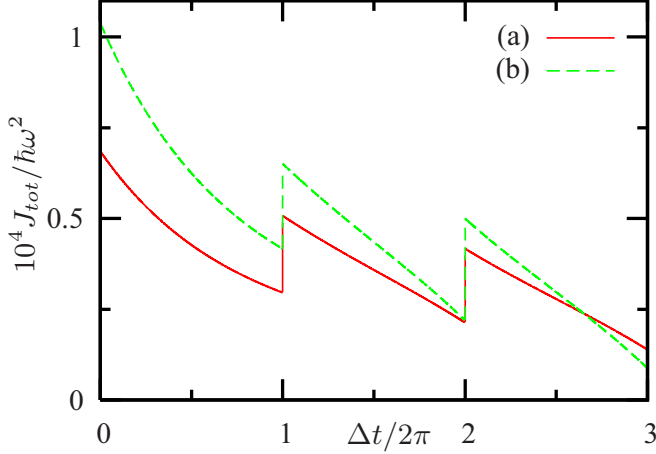FIG. 6. Same as in Fig. 5 for $T_L = 100$ K.

FIG. 7. Energy currents $J_0^{(12)}(t)$ at $T_L = 300$ K: (a) $\hat{\gamma}/\omega = 0.1$ and (b) $\hat{\gamma}/\omega = 0.16$.

The same calculations with $N_B = 1.7 \times 10^6$ modify the values of K by less than 1%, showing convergence of our results. Thus, for $\omega = 460$ cm^{-1}, the total range of K is between 10^{-13} and 10^{-11} W/K, depending on the temperature. These very small values for the thermal conductance are expected due to the narrow channels for thermal transport provided by the molecules. As one can expect, any K in the current case is smaller than the corresponding K_0: phonons traveling across the nanojunction suffer additional reflections from the nanoparticles.

V. CONCLUSIONS

We investigated energy transport in a chain consisting of two macroscopic contacts and two equal nanoparticles interconnected by molecules, shown in Fig. 1. The nanoparticles and contacts are represented by ensembles of harmonic oscillators, and the interaction in the system is described by the Drude-Ullersma model. The macroscopic nature of the contacts in our closed system is simulated by a large ratio $\Delta/\Delta_B = n$ with an integer $n \gg 1$, where Δ and Δ_B are the mode spacing constants for the nanoparticles and contacts. As is shown, the eigenmode spectrum of our system can be
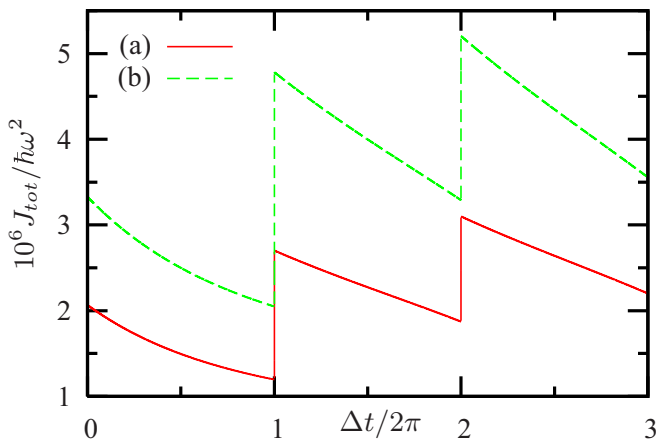

FIG. 8. Same curves as in Fig. 7 for $T_L = 100$ K.

presented as a unification of two subsets. One subset is associated with the contacts and the other one with the nanoparticles. Equations that determine temporal variation of the eigenmode average energies of the contacts and nanoparticles are derived and solved. This allows us to compute the energy current $J_B^{(12)}$ that exits (enters) the contacts and the current $J^{(12)}(t)$ between the nanoparticles. The latter current takes into account energy accumulation by (depletion from) the nanoparticles. As our numerical analysis shows, on the timescale $\Delta^{-1} \lesssim t \ll \Delta_B^{-1}$, $J_B^{(12)}$ is essentially the same as if the contacts' temperatures stay unchanged and equal to their thermal equilibrium values before interconnecting of the chain. On the other hand, despite the presence of the macroscopic contacts, $J^{(12)}(t)$ shows reversibility (or quasiperiodicity) features and peculiarities at time moments $2\pi\ell/\Delta$, with $\ell = 0, 1, 2,...$, representing the finite size effects similar to those in [50]. This is illustrated in Figs 3–6, including the case when the model parameters are taken from the experiment [56]. Substitution of the quasiperiodicity for the true periodicity with period $2\pi/\Delta$ is due to interaction of the nanoparticles with the molecules that inhomogeneously shift uniformly spaced modes [see (15)]. As one can expect, all energy currents increase with the increase of the coupling constants and temperature. An expression for the thermal conductance of the whole nanojunction is derived and evaluated for different temperatures with the experimental parameters [56]. Small values for the thermal conductance are due to the molecules providing narrow channels for the currents and additional phonon reflections from the nanoparticles. This is in a qualitative agreement with the experiment [57], where it was proved that the thermal conductance is not sensitive to the shape of the nanojunction but only to its nanojunction-substrate contacts with the smallest cross section (determined by the molecules in our case), decreasing with the cross section area. A possible experimental study of this kind of system is not necessary to conduct in the nanojunction described here. One can expect that a similar type of size effects can be found also in a nanojunction with only one nanoparticle connected to the contacts by molecules, which is more amenable to experimental study. In this regard, our approach can be easily extended to explore the energy currents and thermal conductance in this kind of nanojunction, as well as for chains of more than two nanoparticles.

APPENDIX A

The interaction matrix of $\mathcal{H}_{tot}$ can be arranged in such a way that, except for its diagonal terms, the only nonzero matrix elements occupy the first three lines and rows. The resulting dispersion equation is factorized $h(z) \cdot H(z) = 0$, where

$$h(z) = \omega^2 - z^2 + 2CS(z)z^2 - \frac{2C_r C_B [S(z)z^2]^2}{H(z)} \quad \text{(A1)}$$

and $H(z) = \Omega^2 - z^2 + [C_r S(z) + C_B S_B(z)]z^2$. Here

$$C = \frac{2\hat{\gamma}D^2}{\pi}, \quad C_r = \frac{2\hat{\gamma}'D^2}{\pi}, \quad C_B = \frac{2\hat{\gamma}_B D_B^2}{\pi}, \quad \hat{\gamma}' = \frac{\gamma'}{M}, \quad \text{(A2)}$$

$$S(z) = \sum_{i=1}^{N} \frac{\Delta}{(\omega_i^2 + D^2)(z^2 - \omega_i^2)}, \quad \text{(A3)}$$

and $S_B(z)$ can be found from $S(z)$ by substitution,

$$N, \Delta, \omega_i, D \rightarrow N_B, \Delta_B, \omega_{Bi}, D_B. \quad \text{(A4)}$$

Thus, we have two separate systems of eigenstates. The first one comes from solving the equation $h(z) = 0$, and the other one comes from solving $H(z) = 0$. In the $h(z) = 0$ case, each eigenfrequency z_k is associated with the eigenvector

$$e^k = e_{0k}\big[1, -d_k, -d_k, E_i(z_k)\big|_{i=1}^{N}, E_i(z_k)\big|_{i=1}^{N},$$
$$E_{Bi}(z_k)\big|_{i=1}^{N_B}, E_{Bi}(z_k)\big|_{i=1}^{N_B}\big], \quad \text{(A5)}$$

where $E_i(z_k) = (rd_k - 1)A_i/(z_k^2 - \omega_i^2)$, $E_{Bi}(z_k) = d_k A_{Bi}/(z_k^2 - \omega_{Bi}^2)$, and $d_k = \sqrt{CC_B}S(z_k)z_k^2/H(z_k)$. In the $H(z) = 0$ case, each z_k is associated with the eigenvector

$$e_H^k = e_{1k}\big[0, 1, -1, -E_i'(z_k)\big|_{i=1}^{N}, E_i'(z_k)\big|_{i=1}^{N},$$
$$-E_{Bi}'(z_k)\big|_{i=1}^{N_B}, E_{Bi}'(z_k)\big|_{i=1}^{N_B}\big], \quad \text{(A6)}$$

where $E_i'(z_k) = rA_i/(z_k^2 - \omega_i^2)$ and $E_{Bi}'(z_k) = A_{Bi}/(z_k^2 - \omega_{Bi}^2)$. In Eqs. (A5) and (A6),

$$A_i = \omega_i\sqrt{\frac{C\Delta}{(\omega_i^2 + D^2)}}, \quad A_{Bi} = \omega_{Bi}\sqrt{\frac{C_B\Delta_B}{(\omega_{Bi}^2 + D_B^2)}}, \quad \text{(A7)}$$

and e_{0k}, e_{1k} are the normalization constants. The first three components of the eigenvectors e_i^k and e_{Hi}^k contribute to the eigenmode expansion for x_C, x_L, and x_R, respectively [see (B1) in Appendix B]. The next $2N$ and last $2N_B$ components of (A5) and (A6) contribute to x_{vi} ($v = 1$ or 2) and $x_{\mu i}$ ($\mu = L$ or R), respectively. As our study shows, the antisymmetric structure of the eigenvectors in the $H(z) = 0$ case can be interpreted in a way where the central molecule stays motionless ($x_C = 0$), whereas symmetrically placed atoms in the nanoparticles and contacts move in opposite directions. In such a case, a study of the whole system breaks into a study of two separate identical problems. Each of them consists of energy transport between the left (right) contact and nanoparticle mediated by a molecule (left or right). Here, we concentrate our attention only on the first case corresponding to the eigenvectors (A5). The roots of $h(z) = 0$ can be found numerically. In our study, $N \sim 10^3$ whereas $N_B > 10^5$. In order to make the numerics feasible we, first of all, present (A3) as

$$S(z) = \frac{1}{z^2 + D^2}\left[\sum_{i=1}^{N}\frac{\Delta}{z^2 - \omega_i^2} + \sum_{i=1}^{N}\frac{\Delta}{\omega_i^2 + D^2}\right] \quad \text{(A8)}$$

and $S_B(z)$ by the same expression (A8) with substitution (A4). The second sum in (A8) can be calculated accurately (it does

not depend on z). Using an accurate relation [58],

$$\sum_{i=1}^{N}\frac{\Delta}{z^2 - \omega_i^2} = \frac{1}{2z}\{\psi(-zN/z_m) - \psi(zN/z_m)$$
$$+ \psi[N(1 + z/z_m) + 1]$$
$$- \psi[N(1 - z/z_m) + 1]\} - \frac{z_m}{z^2 N}, \quad \text{(A9)}$$

the following properties of the first derivative $\psi(z) = \Gamma'(z)$ of the Γ function [58,59],

$$\psi(z + 1) = \psi(z) + \frac{1}{z}, \quad \psi(1 - z) = \psi(z) + \pi \text{ctg}(\pi z), \quad \text{(A10)}$$

and large $|z|$ expansion of $\psi(z)$ [59], one finds

$$z^2 S(z) \approx \frac{\pi z \text{ctg}(\pi N \alpha_z) + 2(P_1 + P_2)}{2(D^2 + z^2)}, \quad \alpha_z = \frac{z}{z_m}, \quad \text{(A11)}$$

$$P_1(z) = z^2 \sum_{i=1}^{N}\frac{\Delta}{\omega_i^2 + D^2} + \frac{z}{2}\ln\left(\frac{1 + \alpha_z}{1 - \alpha_z}\right)$$
$$- \frac{\Delta}{2a_z} + \frac{z\alpha_z}{6(Na_z)^2}\left[1 - \frac{1 + \alpha_z^2}{5(Na_z)^2}\right] \quad \text{(A12)}$$

with $a_z = 1 - \alpha_z^2$, and

$$P_2(z) = \frac{z}{480}\left[\frac{20}{21}\left(\frac{1}{N_m^6} - \frac{1}{N_p^6}\right) + \frac{1}{N_m^8} - \frac{1}{N_p^8}\right], \quad \text{(A13)}$$

where $N_{p,m} = N(1 \pm \alpha_z)$, for the nanoparticles and the similar expression for $z^2 S_B(z)$ with substitution (A4). Formula (A11) works extremely well for all roots z_k except few last roots closest to z_m (or to z_{Bm}). This approximation allows one to decrease the numerical complexity of the problem of finding the roots by 4 orders of magnitude. Using the above approximation, one can express $z^2 S_B(z)$ from the equation $h(z) = 0$ and, looking for the roots in the form $z_k = \Delta_B(k - \phi_k)$, present the resulting equation for finding ϕ_k as

$$\phi_k = \frac{1}{\pi}\text{atan}\left\{\frac{\pi z_k}{2[F_B(z_k) + P_B(z_k)]}\right\}, \quad \text{(A14)}$$

where

$$F_B(z) = \frac{F_\Omega(z)F_{B1}(z) + C_r F_C(z)z^2 S(z)}{F_{B1}(z)F_{B2}(z)}, \quad \text{(A15)}$$

$F_{B1}(z) = F_C(z) + 2Cz^2 S(z)$, and $F_{B2}(z) = C_B/(D_B^2 + z^2)$ with $F_C(z) = \omega^2 - z^2$, $F_\Omega(z) = \Omega^2 - z^2$, and P_B can be obtained from P by substitution (A4) and $z_m \rightarrow z_{Bm}$. Equation (A14) can be solved iteratively on each interval $(i - 1)\Delta_B < z < i\Delta_B$, where $i = 1, 2, ..., N_B$, to find all N_B roots $z_k \equiv z_{Bk}$ that can be associated with the contacts. Convergence is fast and stable. The roots of $h(z) = 0$ can be also found by the bisection method on each interval $(i - 1)\Delta_B < z < i\Delta_B$, $i = 1, 2, ..., N_B$. In this way, one can reproduce exactly the same N_B roots $\{z_{Bk}\}|_{k=1}^{N_B}$ as above and find additional N roots $\{z_k\}|_{k=1}^{N}$, each of them different from any contact root. One can also try to find these N roots by expressing $z^2 S(z)$ from $h(z) = 0$, looking for the roots in the form $z_k = \Delta(k - \phi_k)$, and trying to find ϕ_k iteratively on each interval $(i - 1)\Delta < z < i\Delta$, where $i = 1, 2, ..., N$. In most cases, indeed, a solution found

iteratively in this way coincides with the corresponding root found by the bisection method. In some cases, however, there is no conversion or an iterative solution converges to a wrong value. So, we adopted a different way to find the nanoparticle's roots. We find all roots of $h(z) = 0$ using the bisection method on each interval $(i-1)\Delta_B < z < i\Delta_B$, where $i = 1, 2, ..., N_B$. For most intervals, there is only one (iterative) root. If there are two roots, we distinguish the one coinciding with the iterative root previously found, so the other one is identified as a root associated with the nanoparticles.

Formal solutions of the Heisenberg equations for the contacts' and nanoparticles' operators are

$$x_{\mu i}(t) = x_{\mu i}(0)\cos(\omega_{Bi}t) + \frac{p_{\mu i}(0)}{m_{Bi}\omega_{Bi}}\sin(\omega_{Bi}t)$$
$$+ \frac{C_{Bi}}{m_{Bi}\omega_{Bi}}\int_0^t \sin[\omega_{Bi}(t-s)]x_\mu(s)ds, \quad \text{(A16)}$$

and $p_{\mu i}(t) = m_{Bi}\dot{x}_{\mu i}(t)$, where $\mu = $ L or R;

$$x_{\nu i}(t) = x_{\nu i}(0)\cos(\omega_i t) + \frac{p_{\nu i}(0)}{m_i\omega_i}\sin(\omega_i t)$$
$$+ \frac{C_i}{m_i\omega_i}\int_0^t \sin[\omega_i(t-s)]x_C(s)ds$$
$$+ \frac{C_{ri}}{m_i\omega_i}\int_0^t \sin[\omega_i(t-s)]x_{\mu(\nu)}(s)ds \quad \text{(A17)}$$

and $p_{\nu i}(t) = m_i\dot{x}_{\nu i}(t)$. Here and below $\nu = 1, 2, \mu(1) = $ L, and $\mu(2) = $ R. Excluding $x_{\mu i}$ and $x_{\nu i}$ from the corresponding equations for $x_{L,R,C}$, one obtains three equations that contain only the displacement operators of the molecules. Solving them using the Laplace transform and its inverse in a standard way (see, for example, [17]), one arrives at the following solution for the displacement operator of the central molecule:

$$x_C(t) = x_{C0}(t) + \frac{1}{m}\int_0^t ds g_0(t-s)[\eta_1(s) + \eta_2(s)]$$
$$- \frac{1}{M}\int_0^t ds g_1(t-s)\{r[\eta_1(s) + \eta_2(s)]$$
$$+ \eta_L(s) + \eta_R(s)\}.$$

Here a function $g_0(t)$ (solution kernel) is determined using the Heaviside expansion theorem:

$$g_0(t) = \frac{1}{2\pi i}\int_{c-i\infty}^{c+i\infty} \frac{e^{zt}}{\hat{h}(z)} = \sum_k \frac{e^{\tilde{z}_k t}}{\frac{d}{dz}\hat{h}(z)|_{z=\tilde{z}_k}}, \quad \text{(A18)}$$

where $\tilde{z}_k$ is a root of $\hat{h}(z) = 0$ and $\hat{h}(iz) = h(z)$ from (A1). Taking into account that all the roots of the even function $\hat{h}(z)$ are on the imaginary axis of the z plane, $\tilde{z}_k = iz_k$, one finds

$$g_0(t) = -2\sum_{k=1}^{N_{tot}} \frac{\sin(z_k t)}{h'(z_k)}, \quad \text{where } h'(z) \equiv \frac{d}{dz}h(z). \quad \text{(A19)}$$

Analogously, one can find

$$g_1(t) = -2\sum_{k=1}^{N_{tot}} \frac{f(z_k)\sin(z_k t)}{h'(z_k)} \quad \text{(A20)}$$

with $f(z) = \sqrt{MCC_r/m}S(z)z^2/H(z)$. In a similar way,

$$x_\mu(t) = x_{\mu 0}(t) + \frac{1}{M}\int_0^t ds g_3(t-s)[\eta_1(s) + \eta_2(s)]$$
$$+ \frac{1}{M}\int_0^t ds g_2(t-s)[\eta_L(s) + \eta_R(s)] \quad \text{(A21)}$$

for the left and right molecules, where

$$g_2(t) = -2CC_B R^{-2}\sum_{k=1}^{N_{tot}} \frac{[f(z_k)]^2\sin(z_k t)}{h'(z_k)}, \quad \text{(A22)}$$

$R^2 = M/m$, and $g_3(t) = rg_2(t) - g_1(t)$. Next,

$$\eta_\nu(t) = \sum_{i=1}^{N} C_i\left[x_{\nu i}(0)\cos(\omega_i t) + \frac{p_{\nu i}(0)}{m_i\omega_i}\sin(\omega_i t)\right] \text{ and}$$

$$\eta_\mu(t) = \sum_{i=1}^{N_B} C_{Bi}\left[x_{\mu i}(0)\cos(\omega_{Bi}t) + \frac{p_{\mu i}(0)}{m_{Bi}\omega_{Bi}}\sin(\omega_{Bi}t)\right]$$

are "random forces" or "noises" coming from νth nanoparticle and μth contact. Finally, $x_{C0}(t)$ and $x_{\mu 0}(t)$ depend linearly on the solution kernels and their time derivatives and can be dropped from $x_C(t)$ and $x_\mu(t)$ solutions. Indeed, as our numerics shows, solution kernels $g_q(t)$, where $q = 0, 1, 2,...,$ differ noticeably from zero only on time intervals of the order of $\tau \ll \Delta^{-1}$ in a vicinity of $t = \ell P$, where $P = 2\pi/\Delta$ and $\ell = 0, 1, 2,....$ This is not unusual, because solution kernels usually possess short (on the microscopic scale) memories.

APPENDIX B

The dynamics of $x_{\epsilon i}$ and $p_{\epsilon i}$ is determined by [17,50,51]

$$x_{\epsilon i}(t) = \sum_k \sqrt{\frac{\hbar}{2m_{\epsilon i}z_k}}e_{\epsilon i}^k(a_{\epsilon k}^+ e^{iz_k t} + a_{\epsilon k}e^{-iz_k t}), \quad \text{(B1)}$$

and $p_{\epsilon i}(t) = m_{\epsilon i}\dot{x}_{\epsilon i}(t)$, where $\epsilon i \equiv \epsilon = $ C, L, or R correspond to the central, left, or right molecule, respectively; $\epsilon = \nu = 1$ or 2 with $i = 1, 2, ..., N$ corresponding to the left or right nanoparticles; $\epsilon = \mu = $ L or R with $i = 1, 2, ..., N_B$ corresponding to the left or right contacts. Corresponding components of $e_{\epsilon i}^k$ are determined by (A5).

After the diagonalization, the total system consists of independent modes, each of them carrying eigenenergy $E_{\epsilon k} \equiv \hbar z_k n_{\epsilon k}/2$, where $n_{\epsilon k} = \langle a_{\epsilon k}^+ a_{\epsilon k} + a_{\epsilon k}a_{\epsilon k}^+\rangle$ is the occupation number of the corresponding state. Our goal is to derive equations to find all the (unknown) $E_{\epsilon k}$. This can be done by substituting (B1) and $p_{\epsilon i}(t) = m_{\epsilon i}\dot{x}_{\epsilon i}(t)$ into Eqs. (16)–(19). In this derivation, one can drop contributions proportional to $a_{\epsilon k}^+ a_{\epsilon k_1}^+ \exp[i(z_k + z_{k_1})t]$ and $a_{\epsilon k}a_{\epsilon k_1}\exp[-i(z_k + z_{k_1})t]$ yielding zero at time averaging due to their fast time dependences. In fact, these terms must be also dropped for another reason: due to the absence of any nonlinear interaction in our system, the number of the eigenmodes (phonons) cannot be increased or decreased and is equal to $N_B + N$ [see (14)]. Also, due to the eigenmode independence, only $k_1 = k$ terms survive in the

resulting double sum over k, k_1, and

$$\sum_{i=1}^{N_B} \left\langle \frac{p_{\mu i}^2}{2 m_{Bi}} + \frac{m_{Bi} \omega_{Bi}^2 x_{\mu i}^2}{2} \right\rangle = \sum_k f_{Bk} E_{\mu k} \quad (B2)$$

results. The expression for f_{Bk} follows from (A5):

$$f_{Bk} = \sum_{i=1}^{N_B} \left(e_{Bi}^k\right)^2 = C_B d_k^2 e_{0k}^2 Z_{Bk} \quad \text{with} \quad (B3)$$

$$Z_{Bk} = \sum_{i=1}^{N_B} \frac{\Delta_B \omega_{Bi}^2}{\left(\omega_{Bi}^2 + D_B^2\right)\left(z_k^2 - \omega_{Bi}^2\right)^2}$$

$$\approx \frac{\pi^2}{4 \Delta_B \left(z_k^2 + D_B^2\right) \sin^2(\pi z_k / \Delta_B)} \quad (B4)$$

(see [58]), where $\sin^2(\pi z_k / \Delta_B) = \sin^2(\pi \phi_k)$. As our numerics shows, the relative error of this approximation is $\lesssim 10^{-5}$ for $N_B \gtrsim 10^5$. With the same accuracy,

$$\sum_{i=1}^{N_B} \left(\omega_{Bi} e_{Bi}^k\right)^2 \approx z_k^2 \sum_{i=1}^{N_B} \left(e_{Bi}^k\right)^2 \approx z_k^2 f_{Bk}. \quad (B5)$$

Using a similar approach, one finds

$$\sum_{i=1}^{N} \left\langle \frac{p_{\nu i}^2}{2 m_i} + \frac{m_i \omega_i^2 x_{\nu i}^2}{2} \right\rangle = \sum_k f_{nk} E_{\nu k} \quad \text{with} \quad (B6)$$

$$f_{nk} = \sum_{i=1}^{N} \left(e_{ni}^k\right)^2 = C(r d_k - 1)^2 e_{0k}^2 Z_{nk}. \quad (B7)$$

Here Z_{nk} is determined by (B4) with substitution reverse to (A4), i.e., N_B, Δ_B, ω_{Bi}, $D_B \rightarrow N$, Δ, ω_i, D. Now $N \sim 10^3$ so the relative error of the produced expression for Z_{nk} and the similar to (B5) relation is $\sim 10^{-3}$. This is still good enough for our semi-phenomenological model.

Derivation of the right-hand side in (16), as well as ensemble averages $\mathcal{P}_{C\nu}$ and $\mathcal{P}_{\mu(\nu)\nu}$ in (17), follows similar ideas. Employing (B1), one finds the following for the nanoparticles and contacts:

$$\langle x_{\epsilon i}(0) x_{\epsilon j}(0) + x_{\epsilon j}(0) x_{\epsilon i}(0) \rangle$$

$$= \frac{\hbar}{\sqrt{m_{\epsilon i} m_{\epsilon j}}} \sum_k \frac{n_{\epsilon k} e_{\epsilon i}^k e_{\epsilon j}^k}{z_k} = \frac{2}{\sqrt{m_{\epsilon i} m_{\epsilon j}}} \sum_k \frac{E_{\epsilon k} e_{\epsilon i}^k e_{\epsilon j}^k}{z_k^2}, \quad (B8)$$

$$\langle p_{\epsilon i}(0) p_{\epsilon j}(0) + p_{\epsilon j}(0) p_{\epsilon i}(0) \rangle$$

$$= \hbar \sqrt{m_{\epsilon i} m_{\epsilon j}} \sum_k n_{\epsilon k} z_k e_{\epsilon i}^k e_{\epsilon j}^k = 2 \sqrt{m_{\epsilon i} m_{\epsilon j}} \sum_k E_{\epsilon k} e_{\epsilon i}^k e_{\epsilon j}^k, \quad (B9)$$

and $\langle x_{\epsilon i}(0) p_{\epsilon i}(0) + p_{\epsilon i}(0) x_{\epsilon i}(0) \rangle = 0$. Eventually, the balance equations (16) and (17) can be presented as $\sum_k f_{Bk} \dot{E}_{\mu k} = \sum_k j_{\mu k}$ and $\sum_k f_{nk} \dot{E}_{\nu k} = \sum_k j_{\nu k}$, respectively, where $k = 1, 2, ..., N_B + N$. In order to satisfy them, it is enough to solve $\dot{E}_{\mu k} = j_{\mu k} f_{Bk}^{-1}$ and $\dot{E}_{\nu k} = j_{\nu k} f_{nk}^{-1}$ for each k, resulting in the

following independent sets of four equations for each k:

$$\dot{E}_{Lk}^{B,n} \equiv \frac{d E_{Lk}^{B,n}}{dt} = \mathcal{P}_{BLk}^{B,n} = (F_{Bk} + R_{Bk}) E_{Lk}^{B,n}$$
$$+ R_{nk}\left(E_{1k}^{B,n} + E_{2k}^{B,n}\right) + R_{Bk} E_{Rk}^{B,n} \quad (B10)$$

and $\dot{E}_{Rk}^{B,n} = \mathcal{P}_{BRk}^{B,n}$, with $\mathcal{P}_{BRk}^{B,n}$ produced from $\mathcal{P}_{BLk}^{B,n}$ by exchange $E_{Lk}^{B,n} \leftrightarrow E_{Rk}^{B,n}$. For nanoparticles,

$$\dot{E}_{1k}^{B,n} = \mathcal{P}_{C1k}^{B,n} + \mathcal{P}_{L1k}^{B,n} \quad \text{and} \quad \dot{E}_{2k}^{B,n} = \mathcal{P}_{C2k}^{B,n} + \mathcal{P}_{R2k}^{B,n}, \quad (B11)$$

where

$$\mathcal{P}_{C1k}^{B,n} = (F_{nk}' + R_{nk}') E_{1k}^{B,n} + R_{nk}' E_{2k}^{B,n} + R_{Bk}'\left(E_{Lk}^{B,n} + E_{Rk}^{B,n}\right), \quad (B12)$$

$$\mathcal{P}_{L1k}^{B,n} = (F_{nk}'' + R_{nk}'') E_{1k}^{B,n} + R_{nk}'' E_{2k}^{B,n} + R_{Bk}''\left(E_{Lk}^{B,n} + E_{Rk}^{B,n}\right), \quad (B13)$$

and $\mathcal{P}_{C2k}^{B,n}$ and $\mathcal{P}_{R2k}^{B,n}$ are produced from $\mathcal{P}_{C1k}^{B,n}$ and $\mathcal{P}_{L1k}^{B,n}$ by exchange $E_{1k}^{B,n} \leftrightarrow E_{2k}^{B,n}$. Here the superscripts B and n mean that $z_k \in \{z_{Bk}\}_{k=1}^{N_B}$ and $z_k \in \{z_{nk}\}_{k=1}^{N}$, respectively. Finally, considering $\dot{E}_{Lk}^{B,n} - \dot{E}_{Bk}^{B,n}$ in (B10) and $\dot{E}_{1k}^{B,n} - \dot{E}_{2k}^{B,n}$ in (B11), one arrives at (22)–(24).

The coefficients F and R in (B10)–(B13) are not all independent. Relations between them follow from the energy conservation law for our closed system applied for each eigenstate:

$$\mathcal{P}_{BLk}^{B,n} + \mathcal{P}_{BRk}^{B,n} + \mathcal{P}_{C1k}^{B,n} + \mathcal{P}_{L1k}^{B,n} + \mathcal{P}_{C2k}^{B,n} + \mathcal{P}_{R2k}^{B,n} = 0. \quad (B14)$$

Using here the right-hand sides of Eqs. (B10)–(B13) and taking into account that (B14) must be correct for any initial eigenstate average energy (for any initial temperatures), one can derive the following relations:

$$D_{k1} \equiv F_{Bk} + 2(R_{Bk} + R_{Bk}' + R_{Bk}'') = 0 \quad (B15)$$

and

$$D_{k2} \equiv F_{nk}' + F_{nk}'' + 2(R_{nk} + R_{nk}' + R_{nk}'') = 0. \quad (B16)$$

Equations (B10)–(B13) assume that there is no energy accumulation (depletion) by the molecules on the timescale Δ^{-1}. We were able to confirm this explicitly by computing the rate of energy variation of the molecules as it was done in (16) and (17) with substituting $\mathcal{H}_{B\mu}$ or $\mathcal{H}_{n\nu}$ by $\mathcal{H}_{M\sigma}$.

As one can notice, $\mathcal{P}_{LBk}^{B,n} = -\mathcal{P}_{BLk}^{B,n}$ can be considered as the kth eigenmode energy current flowing from the left contact towards the left nanoparticle. Thus, the kth contribution to the energy current flowing between the nanoparticles is

$$J_k^{(12)} = \mathcal{P}_{LBk}^{B,n} - \left(\mathcal{P}_{L1k}^{B,n} + \mathcal{P}_{C1k}^{B,n}\right), \quad (B17)$$

which takes into account that the current exiting from the left contact is partially absorbed (or augmented) by the left nanoparticle by the amount indicated inside the brackets before it reaches the central molecule. Similarly, the kth energy current that reaches the central molecule from the right is

$$J_k^{(21)} = \mathcal{P}_{RBk}^{B,n} - \left(\mathcal{P}_{R2k}^{B,n} + \mathcal{P}_{C2k}^{B,n}\right) = -J_k^{(12)}, \quad (B18)$$

where $\mathcal{P}_{RBk}^{B,n} = -\mathcal{P}_{BRk}^{B,n}$. The last relation in (B18) is due to (B14). Using (B10)–(B17), one arrives at (25)–(27).

The expression for F_{Bk} appears after substitution of the nonintegral part of $p_{\mu i}(t) = m_{Bi}\dot{x}_{\mu i}(t)$ with $x_{\mu i}(t)$ from (A16) and the integral part of x_μ from (A21) into (16). The result is

$$P_{B\mu} = \frac{1}{2}\int_0^t ds g_2(t-s)[S_{\mu a} - S_{\mu b}], \quad \text{where} \quad \text{(B19)}$$

$$S_{\mu a} = \sum_{i=1}^{N_B}\frac{C_{Bi}\cos(\omega_{Bi}t)}{Mm_{Bi}f_{Bk}}\langle\eta_\mu(s)p_{\mu i}(0) + p_{\mu i}(0)\eta_\mu(s)\rangle$$

and

$$S_{\mu b} = \sum_{i=1}^{N_B}\frac{C_{Bi}\omega_{Bi}\sin(\omega_{Bi}t)}{Mf_{Bk}}\langle\eta_\mu(s)x_{\mu i}(0) + x_{\mu i}(0)\eta_\mu(s)\rangle.$$

Using the expression for η_μ (end of Appendix A) and Eqs. (B8) and (B9) results in

$$\langle\eta_\mu(s)p_{\mu i}(0) + p_{\mu i}(0)\eta_\mu(s)\rangle$$
$$= 2\sqrt{m_{Bi}}\sum_{j=1}^{N_B}\frac{C_{Bj}\sin(\omega_{Bj}s)}{\sqrt{m_{Bj}}\omega_{Bj}}\sum_{k=1}^{N_B}e_{Bi}^k e_{Bj}^k E_{\mu k}(s) \quad \text{and} \quad \text{(B20)}$$

$$\langle\eta_\mu(s)x_{\mu i}(0) + x_{\mu i}(0)\eta_\mu(s)\rangle$$
$$= \frac{2}{\sqrt{m_{Bi}}}\sum_{j=1}^{N_B}\frac{C_{Bj}\cos(\omega_{Bj}s)}{\sqrt{m_{Bj}}}\sum_{k=1}^{N_B}e_{Bi}^k e_{Bj}^k z_k^{-2}E_{\mu k}(s). \quad \text{(B21)}$$

Substituting (B20) into $S_{\mu a}$ and (B21) into $S_{\mu b}$, one finds

$$S_{\mu a} = 2C_B\sum_{k=1}^{N_B}E_{\mu k}(s)Z_{Bk}^{-1}\sum_{i=1}^{N_B}b_i^k\omega_{Bi}^2\cos(\omega_{Bi}t)$$
$$\times\sum_{j=1}^{N_B}b_j^k\omega_{Bj}\sin(\omega_{Bj}s) \quad \text{and}$$

$$S_{\mu b} = 2C_B\sum_{k=1}^{N_B}E_{\mu k}(s)z_k^{-2}Z_{Bk}^{-1}\sum_{i=1}^{N_B}b_i^k\omega_{Bi}^3\sin(\omega_{Bi}t)$$
$$\times\sum_{j=1}^{N_B}b_j^k\omega_{Bj}^2\cos(\omega_{Bj}s),$$

where $b_i^k = \Delta_B/[(\omega_{Bi}^2 + D_B^2)(z_k^2 - \omega_{Bi}^2)]$. Defining

$$B_{Bk}(t) \equiv \sum_{i=1}^{N_B}b_i^k\sin(\omega_{Bi}t), \quad \text{(B22)}$$

$A_{Bk}(t) = \dot{B}_{Bk}(t)$, and $\dot{A}_{Bk}(t) = G(t) - z_k^2 B_{Bk}(t)$ with

$$G(t) = \sum_{k=1}^{N_B}\frac{\Delta_B\omega_{Bi}\sin(\omega_{Bi}t)}{\omega_{Bi}^2 + D_B^2}, \quad \text{(B23)}$$

one can write

$$P_{B\mu} = C_B\sum_{i=1}^{N_B}Z_{Bk}^{-1}\int_0^t ds g_2(t-s)E_{\mu k}(s)$$
$$\times[A_{Bk}(t)B_{Bk}(s) - B_{Bk}(t)A_{Bk}(s) + G(t)A_{Bk}(s)]. \quad \text{(B24)}$$

Taking into account that $g_2(t)$ decays fast (see the observation at the end of Appendix A) whereas $E_{Bk}(s)$ varies on a much longer timescale, $E_{Bk}(s)$ can be taken out from the integral at $s = t$ and (B24) can be rewritten as

$$P_{B\mu} \approx \sum_{i=1}^{N_B}E_{\mu k}(t)F_{Bk} \quad \text{with} \quad \text{(B25)}$$

$$F_{Bk}(t) = C_B Z_{Bk}^{-1}[S_{AB}^F(t) - S_{BA}^F(t)], \quad \text{where} \quad \text{(B26)}$$

$$S_{AB}^F(t) = A_{Bk}(t)\int_0^t ds g_2(t-s)B_{Bk}(s), \quad \text{(B27)}$$

and S_{BA}^F can be produced from S_{AB}^F by interchanging $A_{Bk} \leftrightarrow B_{Bk}$. Here we also neglected the $G(t)$ term, because $G(t)$ is fast oscillating and a quickly decaying function of time: as our numerics shows, its contribution to F_{Bk} is less than 1%.

A possible way to compute F_{Bk} is to present it as

$$F_{Bk}(t) = C_B Z_{Bk}^{-1}\sum_{i,j=1}^{N_B}\left[f_i^k\omega_{Bi}f_j^k I_{1ij}(t) - f_i^k f_j^k\omega_{Bj}I_{2ij}(t)\right]$$

using the definitions of A_{Bk} and B_{Bk}. Here $f_i^k = b_i^k\omega_{Bi}$, $I_{1ij}(t) = \cos(\omega_{Bi}t)[\sin(\omega_{Bj}t)g_{2cj} - \cos(\omega_{Bj}t)g_{2sj}]$, and $I_{2ij}(t) = \sin(\omega_{Bi}t)[\cos(\omega_{Bj}t)g_{2cj} + \sin(\omega_{Bj}t)g_{2sj}]$. In accordance to the observation at the end of Appendix A, each time when t passes ℓP, the integrals

$$g_{2cj} \equiv \int_0^t ds g_2(s)\cos(\omega_{Bj}s), \quad g_{2sj} \equiv \int_0^t ds g_2(s)\sin(\omega_{Bj}s)$$

change their values and stay approximately unchanged until the next time moment $(\ell + 1)P$, allowing the following approximation by the step functions $\theta(t)$ on the interval $0 < t \leqslant \ell P$:

$$g_{2c,sj}(t) \approx g_{2c,sj}(1) + \sum_{n=1}^{(\ell-1)}\delta g_{2c,sj}(n)\theta(t - nP) \quad \text{(B28)}$$

with $P = 2\pi/\Delta$, $\delta g_{2c,sj}(n) \equiv g_{2c,sj}(n+1) - g_{2c,sj}(n)$, and

$$g_{2sj}(n) = \frac{1}{P}\int_{(n-1)P}^{nP}dt\int_0^t ds\hat{g}_{2j}(s)$$
$$= \int_0^{(n-1)P}ds\hat{g}_{2j}(s) + \int_{(n-1)P}^{nP}ds(n - s/P)\hat{g}_{2j}(s) \quad \text{(B29)}$$

are the time averages on the interval $(n-1)P \leqslant t \leqslant nP$. Here $\hat{g}_{2j}(s) = g_2(s)\sin(\omega_{Bj}s)$, and $g_{2cj}(n)$ is determined by (B29) with substitution $\sin(\omega_{Bj}s) \to \cos(\omega_{Bj}s)$. Finally, substituting the following products by the corresponding time averages, $\sin(\omega_{Bi}t)\cos(\omega_{Bj}t) \to 0$ and $\sin(\omega_{Bi}t)\sin(\omega_{Bj}t)$, $\cos(\omega_{Bi}t)\cos(\omega_{Bj}t) \to \delta_{i,j}/2$, our $F_{Bk}^{\text{approx}} \equiv F_{Bk}(n)$ on each periodicity interval is found as

$$F_{Bk}(n) = -C_B Z_{Bk}^{-1}\sum_{i=1}^{N_B}\frac{\Delta_B^2\omega_{Bi}^3 g_{2si}(n)}{(\omega_{Bi}^2 + D_B^2)^2(z_k^2 - \omega_{Bi}^2)^2}. \quad \text{(B30)}$$

Simplifying (B30) using a similar to (B4) approach, one finds

$$F_{Bk}(n) = -\frac{C_B \Delta_B z_k g_{2sk}(n)}{z_k^2 + D_B^2}, \quad g_{2sk}(n) = g_{2si}(n)|_{\omega_{Bi} \to z_k}.$$
(B31)

As follows from comparison with its initial (accurate) value (B26), illustrated in Fig. 2, the accuracy of (B31) is good.

Similarly, initially $F'_{nk}(t) = CZ_{nk}^{-1}[S_{AB}^{F'}(t) - S_{BA}^{F'}(t)]$. Here

$$S_{AB}^{F'}(t) = A_{nk}(t) \int_0^t ds\, g_4(t-s) B_{nk}(s),$$

where $g_4(t) = g_0(t) - rg_1(t)$, B_{nk} is found from B_{Bk} reversing (A4), $A_{nk}(t) = \dot{B}_{nk}(t)$, and $F'^{approx}_{nk} \equiv F'_{nk}(n)$, where

$$F'_{nk}(n) = -CZ_{nk}^{-1} \sum_{i=1}^N \frac{\Delta^2 \omega_i^3 g_{4si}(n)}{(\omega_i^2 + D^2)^2 (z_k^2 - \omega_i^2)^2}$$
(B32)

with $g_{4si}(n)$ is obtained from (B29) by the substitution $\hat{g}_{2i}(s) \to \hat{g}_{4i}(s) \equiv g_4(s)\sin(\omega_i s)$.

Finally, initially $F''_{nk}(t) = CrR^{-2}Z_{nk}^{-1}[S_{AB}^{F''}(t) - S_{BA}^{F''}(t)]$ and $S_{AB}^{F''}$ is obtained from $S_{AB}^{F'}$ with $g_4 \to g_3$. Thus, F''^{approx}_{nk} is

$$F''_{nk}(t) = -\frac{Cr}{R^2} Z_{nk}^{-1} \sum_{i=1}^N \frac{\Delta^2 \omega_i^3 g_{3si}(n)}{(\omega_i^2 + D^2)^2 (z_k^2 - \omega_i^2)^2},$$
(B33)

where $g_{3si}(n)$ is obtained from (B29) by the substitution $\hat{g}_{2i}(s) \to \hat{g}_{3i}(s) \equiv g_3(s)\sin(\omega_i s)$.

As one can see, the computational complexities of the initial forms for $F_{Bk}(t)$ and $F'_{nk}(t)$ or $F''_{nk}(t)$ are $O(N_B N_t^2)$ and $O(N N_t^2)$, respectively. For comparison, complexities for the step-function approximations of $F_{Bk}(n)$ and $F'_{nk}(n)$ or $F''_{nk}(n)$ in (B31) and (B32)–(B33) are only $O(N_B N_t)$ and $O(N N_t)$, respectively. Here N_t is the number of mesh points in computing time integrals and $N_t \lesssim 10^5$ in our case. Expressions for the R coefficients appear after substitution of the integral part of $p_{\mu,\nu i}$ into the right-hand sides of (16), (18), or (19). Derivation of these coefficients follows exactly the same ideas and approximations as those described above. In fact, we do not need any R coefficients for computing the energy currents or thermal conductance. Taking into account that $N \ll N_t \lesssim N_B$, the adopted approximation expedites calculation of all F (or R) coefficients by a factor N_t, making the total computational complexity just $O(N_B N_t)$, which is not a problem even for $N_B \sim 10^6$.

[1] M. Galperin, M. A. Ratner, and A. Nitzan, J. Phys.: Condens. Matter **19**, 103201 (2007).

[2] A. Dhar, Adv. Phys. **57**, 457 (2008).

[3] Y. Dubi and M. Di Ventra, Rev. Mod. Phys. **83**, 131 (2011).

[4] V. V. Zhirnov, R. K. Cavin, J. A. Hutchby, and G. I. Bourianoff, Proc. IEEE **91**, 1934 (2003).

[5] G. Cerefolini, *Nanoscale Devices* (Springer, Berlin, 2009).

[6] N. Li, J. Ren, L. Wang, G. Zhang, P. Hanggi, and B. Li, Rev. Mod. Phys. **84**, 1045 (2012).

[7] A. I. Hochbaum, R. Chen, R. D. Delgado, W. Liang, E. C. Garnett, M. Najarian, A. Majumdar, and P. Yang, Nature (London) **451**, 163 (2008).

[8] A. I. Boukai, Y. Bunimovich, J. Tahir-Kheli, J.-K. Yu, W. A. Goddard III, and James R. Heath, Nature (London) **451**, 168 (2008).

[9] C. A. Perroni, D. Ninno, and V. Cataudella, Phys. Rev. B **90**, 125421 (2014).

[10] *Molecular Electronics*, edited by J. Jortner and M. Ratner (Blackwell Science, Oxford, 1997).

[11] P. Hänggi, M. Ratner, and S. Yalikari, Chem. Phys. **281**, 111 (2002).

[12] D. Segal, Phys. Rev. Lett. **100**, 105901 (2008).

[13] D. Segal, Phys. Rev. E **90**, 012148 (2014).

[14] A. O. Caldeira and A. J. Leggett, Physica A **121**, 587 (1983).

[15] Y. L. Klimontovich, *Statistical Theory of Open Systems* (Kluwer, Amsterdam, 1997).

[16] A. E. Allahverdyan and Th. M. Nieuwenhuizen, Phys. Rev. Lett. **85**, 1799 (2000).

[17] Th. M. Nieuwenhuizen and A. E. Allahverdyan, Phys. Rev. E **66**, 036102 (2002).

[18] U. Zürcher and P. Talkner, Phys. Rev. A **42**, 3278 (1990).

[19] K. Saito, S. Takesue, and S. Miyashita, Phys. Rev. E **61**, 2397 (2000).

[20] A. Dhar and B. S. Shastry, Phys. Rev. B **67**, 195405 (2003).

[21] D. Segal, A. Nitzan, and P. Hänggi, J. Chem. Phys. **119**, 6840 (2003).

[22] H. Dammak, Y. Chalopin, M. Laroche, M. Hayoun, and J.-J. Greffet, Phys. Rev. Lett. **103**, 190601 (2009).

[23] M. Basire, D. Borgis, and R. Vuilleumier, Phys. Chem. Chem. Phys. **15**, 12591 (2013).

[24] X. Li, Phys. Rev. E **90**, 032112 (2014).

[25] D. N. Zubarev, Fortschr. Phys. **18**, 125 (1970).

[26] M. Toda, R. Kubo, and N. Hashitsume, *Statistical Physics, II. Nonequilibrium Statistical Mechanics* (Springer, Berlin, 1983).

[27] L. V. Keldysh, Sov. Phys. JETP **20**, 1018 (1965).

[28] C. Caroli, R. Combescot, P. Nozieres, and D. Saint-James, J. Phys. C **4**, 916 (1971).

[29] Y. Meir and N. S. Wingreen, Phys. Rev. Lett. **68**, 2512 (1992).

[30] S. Datta, *Electronic Transport in Mesoscopic Systems* (Cambridge University Press, Cambridge, UK, 1995).

[31] A. Ozpineci and S. Ciraci, Phys. Rev. B **63**, 125415 (2001).

[32] T. Yamamoto and K. Watanabe, Phys. Rev. Lett. **96**, 255503 (2006).

[33] J. S. Wang, N. Zeng, J. Wang, and C. K. Gan, Phys. Rev. E **75**, 061128 (2007).

[34] T. Ojanen and A. P. Jauho, Phys. Rev. Lett. **100**, 155902 (2008).

[35] A. Dhar and D. Roy, J. Stat. Phys. **125**, 805 (2006).

[36] K. Walczak and K. L. Yerkes, J. Appl. Phys. **115**, 174308 (2014).

[37] J. S. Wang, J. Wang, and J. T. Lü, Eur. Phys. J. B **62**, 381 (2008).

[38] T. Prosen, New J. Phys. **10**, 043026 (2008).

[39] T. Prosen and B. Žunkovič, New J. Phys. **12**, 025016 (2010).

[40] J. Thinga, J. S. Wang, and P. Hänggi, J. Chem. Phys. **136**, 194110 (2012).

[41] F. Hache, D. Ricard, and C. Flytzanis, J. Opt. Soc. Am. B **3**, 1647 (1986).

[42] S. G. Rautian, Sov. Phys. JETP **85**, 451 (1997).

[43] G. Y. Panasyuk, J. C. Schotland, and V. A. Markel, Phys. Rev. Lett. **100**, 047402 (2008).

[44] A. A. Govyadinov, G. Y. Panasyuk, J. C. Schotland, and V. A. Markel, Phys. Rev. B **84**, 155461 (2011).

[45] G. Y. Panasyuk, J. C. Schotland, and V. A. Markel, Phys. Rev. B **84**, 155460 (2011).

[46] S. P. Adiga, V. P. Adiga, R. W. Carpick, and D. W. Brenner, J. Phys. Chem. C **115**, 21691 (2011).

[47] D. Sopu, J. Kotakoski, and K. Albe, Phys. Rev. B **83**, 245416 (2011).

[48] J. Pohl, C. Stahl, and K. Albe, Beilstein J. Nanotechnol. **3**, 1 (2012).

[49] E. C. Cuansing, H. Li, and J. S. Wang, Phys. Rev. E **86**, 031132 (2012).

[50] G. Y. Panasyuk and K. L. Yerkes, Phys. Rev. E **87**, 062118 (2013).

[51] G. Y. Panasyuk and K. L. Yerkes, Phys. Rev. E **92**, 062138 (2015).

[52] G. W. Ford, J. T. Lewis, and R. F. O'Connell, Phys. Rev. A **37**, 4419 (1988).

[53] G. Y. Panasyuk, G. A. Levin, and K. L. Yerkes, Phys. Rev. E **86**, 021116 (2012).

[54] P. Ullersma, Physica (Utrecht) **32**, 27 (1966); **32**, 56 (1966); **32**, 74 (1966); **32**, 90 (1966).

[55] U. Weiss, *Quantum Dissipative Systems* (World Scientific, Singapore, 1993).

[56] A. M. Orlov, A. A. Skvortsov, A. G. Klement'ev, and A. V. Sindaev, Tech. Phys. Lett. **27**, 77 (2001).

[57] L. Jalabert, T. Sato, T. Ishida, H. Fujita, Y. Chalopin, and S. Volz, Nanoletters **12**, 5213 (2012).

[58] A. P. Prudnikov, Y. A. Brychkov, and O. I. Marichev, *Integrals and Series: Elementary Functions* (Gordon and Breach, Amsterdam, 1998), Vol. 1.

[59] *Handbook of Mathematical Functions*, edited by M. Abramovich and I. A. Stegun (Dover Publications, Inc., New York, 1972).